

This is a repository copy of *The Impact of Cracks on Photovoltaic Power Performance*.

White Rose Research Online URL for this paper:

<https://eprints.whiterose.ac.uk/177672/>

Version: Accepted Version

---

**Article:**

Dhimish, Mahmoud, Holmes, Violeta, Mehrdadi, Bruce et al. (1 more author) (2017) The Impact of Cracks on Photovoltaic Power Performance. *Journal of Science: Advanced Materials and Devices*. pp. 199-209.

<https://doi.org/10.1016/j.jsamd.2017.05.005>

---

**Reuse**

Items deposited in White Rose Research Online are protected by copyright, with all rights reserved unless indicated otherwise. They may be downloaded and/or printed for private study, or other acts as permitted by national copyright laws. The publisher or other rights holders may allow further reproduction and re-use of the full text version. This is indicated by the licence information on the White Rose Research Online record for the item.

**Takedown**

If you consider content in White Rose Research Online to be in breach of UK law, please notify us by emailing [eprints@whiterose.ac.uk](mailto:eprints@whiterose.ac.uk) including the URL of the record and the reason for the withdrawal request.

# The Impact of Cracks on Photovoltaic Power Performance

## *Abstract*

This paper presents a statistical approach for identifying the significant impact of cracks on the output power performance for photovoltaic (PV) modules. There are a few data statistical analysis for investigating the impact of cracks in PV modules in real-time long-term field data measurements. Therefore, this paper will demonstrate a statistical analysis approach which uses T-test and F-test for identifying whether the crack has a significant or non-significant impact on the total amount of power generated by the PV modules. Electroluminescence (EL) method is used for scanning possible faults in the examined PV modules. However, Virtual Instrumentation (VI) LabVIEW software is used to simulate the theoretical I-V and P-V curves. The approach classified only 60% of cracks that has a significant impact on the total amount of power generated by PV modules.

**Keywords:** Photovoltaic (PV) Module Performance; Solar cell cracks; Statistical Approach; Electroluminescence (EL); Surface Analysis

## *1. Introduction*

Cell cracks appear in the photovoltaic (PV) panels during their transportation from the factory to the place of installation. Also, some climate proceedings such as snow loads, strong winds and hailstorms might create some major cracks on the PV modules surface [1-3]. These cracks may lead to disconnection of cells parts and, therefore, to a loss in the total power generated by the PV modules [4].

There are several types of cracks that might occur in PV modules: diagonal cracks, parallel to busbars crack, perpendicular to busbars crack and multiple directions crack. Diagonal Cracks and multiple directions cracks always show a significant reduction in the PV output power [5].

Moreover, the PV industry has reacted to the in-line non-destructive cracks by developing new techniques of crack detection such as resonance ultrasonic vibration (RUV) for screening PV cells with pre-existing cracks [6]. This helped to reduce cell cracking due to defective wafers, but, it does not mitigate the cracks generated during the manufacturing process of PV modules.

When cracks appear in a solar cell, the parts separated from the cell might not be totally disconnected, but the series resistance across the crack varies as a function of the distance between the cell parts and the number of cycles for which module is deformed [7]. However, when a cell part is fully isolated, the current decrease is proportional to the disconnected area [8, 9].

37 Collecting the data from damaged PV modules using installed systems is a challenging task.  
38 Electroluminescence (EL) imaging method is used to scan the surface of the PV modules, the light  
39 output increases with the local voltage so that regions with poor contact show up as dark spots [10,  
40 11]. The thermography technique is simpler to implement, but the accuracy of the image is lower  
41 than with the EL technique, and does not allow the estimation of the area (in mm<sup>2</sup>) that is broken  
42 in the solar cells [12, 13]. Therefore, in this paper we have used EL imaging method which can be  
43 illustrated and discussed briefly in the following articles [14-16].

44 As proposed in [17] the performance of PV systems can be monitored using virtual instrumentation  
45 software such as LabVIEW. Also MATLAB software allows users to create tools to model,  
46 monitor and estimate the performance of photovoltaic systems. The simulation tool is important  
47 to compare the output measured data from PV module with its own theoretical performance [18].

48 There are a few statistical analysis tools that have been deployed in PV applications. The common  
49 used tool is the normal standard deviation limits ( $\pm 1$  SD or  $\pm 3$  SD) technique [19]. However, [20]  
50 used a statistical local distribution analysis in identifying the type of cracks in a PV modules. To  
51 the best of our knowledge, few of the reviewed articles have used a real-time long-term statistical  
52 analysis approach for PV cracked modules under real-time operational process. Therefore, the  
53 main contribution of this work can be illustrated as the following:

- 54 • Development of a novel statistical analysis approach that can be used to identify the  
55 significant effect of cracks on the output power performance for PV modules under various  
56 environmental field data measurements.
- 57 • Proving that not all cracks has a significant impact on the PV output power performance.

58 This paper is organized as follows: Section 2 describes the methodology used which contains the  
59 data acquisition, PV modules cracks and the statistical analysis approach, while Section 3 lists the  
60 output results of the entire work. The discussion is presented in section 4. Finally, Sections 5 and  
61 6 describes the conclusion and the acknowledgment respectively.

## 62 **2. Methodology**

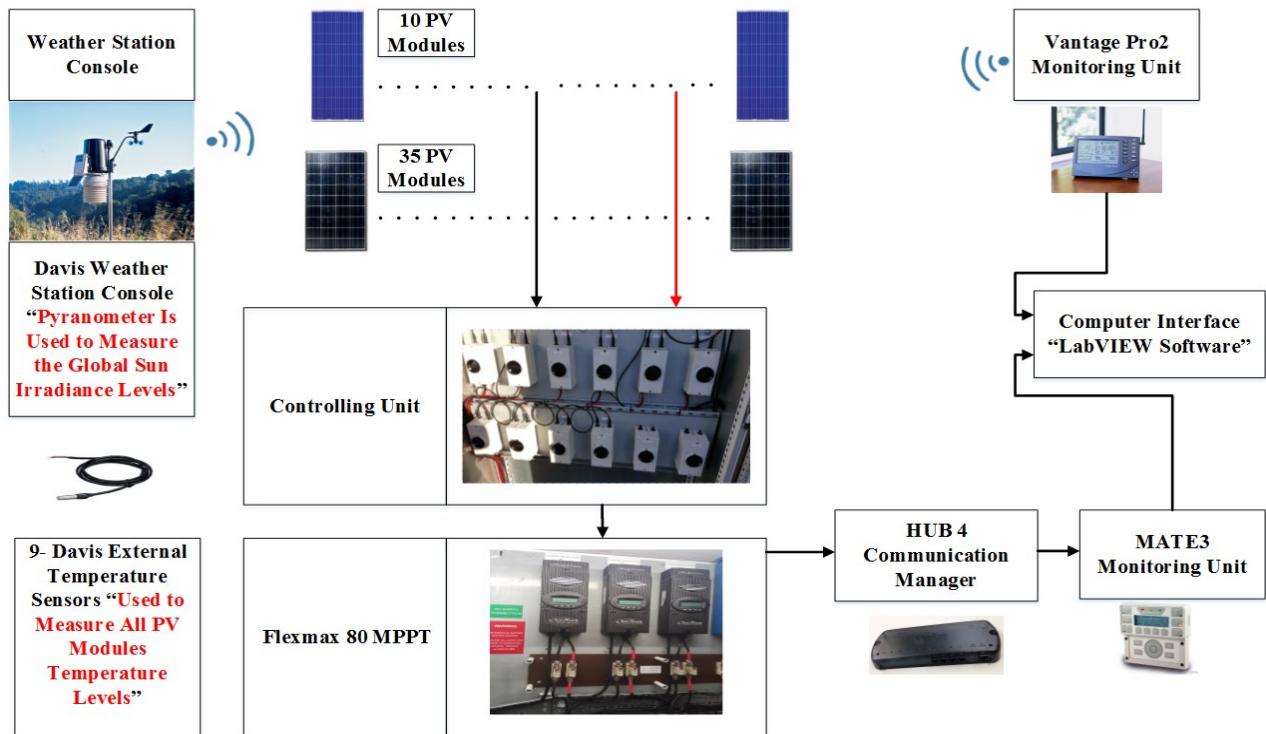
### 63 **2.1. Data acquisition**

64 In this work, we used a statistical study of broken cells showing different crack types. Several test  
65 measurements are carried out on two different PV plants at the University of Huddersfield, United  
66 Kingdom. The first system consists of 10 polycrystalline PV modules with an optimum power  
67 220Wp. However, the second system consists of 35 polycrystalline with 130Wp each. Both  
68 systems are shown in Fig. 1.

69 As presented in Fig. 1(A) and Fig 1(B), there are two examined PV systems with total amount of  
70 PV modules equal to 45. To establish the connection for each PV module separately, a controlling  
71 unit is designed to allow the user to connect any PV module to a FLEXmax 80 MPPT. In order to  
72 facilitate a real-time monitoring for each PV module, therefore, Vantage Pro monitoring unit is  
73 used to receive the Global solar irradiance measured by Davis weather station which includes  
74 pyranometer. Hub 4 communication manager is used to facilitate acquisition of modules  
75 temperature using Davis external temperature sensor, and the electrical data for each photovoltaic

76 module. LabVIEW software is used to implement the data logging and monitoring functions of  
 77 the examined PV modules.

78 Fig. 1(C) shows the data acquisition system. Furthermore, Table I illustrates both electrical  
 79 characteristics of the solar modules that are used in this work. The standard test condition (STC)  
 80 for all examined solar panels are: Solar Irradiance =  $1000 \text{ W/m}^2$ ; Module Temperature =  $25 \text{ }^\circ\text{C}$ .



(C)

Fig. 1. (A) 10 PV Modules (SMT 6 (60) P) with 220W Output Peak Power; (B) 35 PV Modules (KC130 GHT-2) with 130W Output Peak Power; (C) Monitoring the Examined PV System Using LabVIEW Software

TABLE I  
ELECTRICAL CHARACTERISTICS FOR BOTH PV SYSTEMS MODULES

Solar Panel Electrical Characteristics	1 <sup>st</sup> System: PV Module, SMT 6 (60) P	2 <sup>nd</sup> System: PV Module, KC130 GHT-2
Peak Power	220 W	130
Voltage at Maximum Power Point ( $V_{mp}$ )	28.7 V	17.6
Current at Maximum Power Point ( $I_{mp}$ )	7.67 A	7.39
Open Circuit Voltage ( $V_{oc}$ )	36.74 V	21.9
Short Circuit Current ( $I_{sc}$ )	8.24 A	8.02
Number of Cells Connected in Series	60	36
Number of Cells Connected in Parallel	1	1
PV System Tilt Angle and Azimuth Angle (North-South)	42°, 185°	42°, 180°
Davis Pyranometer Sensor Tilt Angle and Azimuth Angles (North-South)	42°, 185°	42°, 180°

## 81 **2.2. Electroluminescence setup and PV modules cracks**

82 The electroluminescence system developed is presented in Fig. 2(A). The system is comprised of  
 83 a light-tight black-box where housed inside is a digital camera and a sample holder. The digital  
 84 camera is equipped with a standard F-mount 18–55 mm lens. To allow for detection in the near  
 85 infrared, the IR filter was removed and replaced with a full spectrum window of equal optical path  
 86 length. In our setup a Nikon D40 was used, but in principle any digital camera with similar grade  
 87 CCD or CMOS sensor and where the IR filter can be removed would serve the purpose. The bias  
 88 was applied and the resultant current and the voltage are measured by a voltage and current sensors  
 89 which are wirelessly connected to the personal computer (PC). The purpose of the PC is to get the  
 90 electroluminescence image of the solar module and predicting the theoretical output power  
 91 performance of the PV module.

92 In order to reduce the noise and increase the accuracy, all EL images are processed by removing  
 93 background noise and erroneous pixels. Firstly, background image has been captured under the  
 94 same conditions as the EL images but without forward biasing the cell. This background image is  
 95 subtracted from each EL image in order to reduce the image noise level. The images are cropped  
 96 to the appropriate size and in the case of high resolution imaging system the captured cell images  
 97 are compiled together to form an image of the entire module. Additionally, to increase the accuracy  
 98 and the vision of the EL image, each PV module cell is captured separately.

99 In order to determine the cracks location, type and size; reflex camera has been used for imaging  
 100 possible cracks in each PV module. As explained previously in the introduction, EL imaging  
 101 technique is used worldwide and it has been demonstrated by many researchers [14-16]. Broken  
 102 cells are sorted according to the type of crack, Fig. 2 shows all examined crack types which are  
 103 classified as the following:

- 104 A. Diagonal crack (+45<sup>0</sup>)
- 105 B. Diagonal crack (- 45<sup>0</sup>)
- 106 C. Parallel to busbars crack
- 107 D. Perpendicular to busbars crack
- 108 E. Multiple directions crack

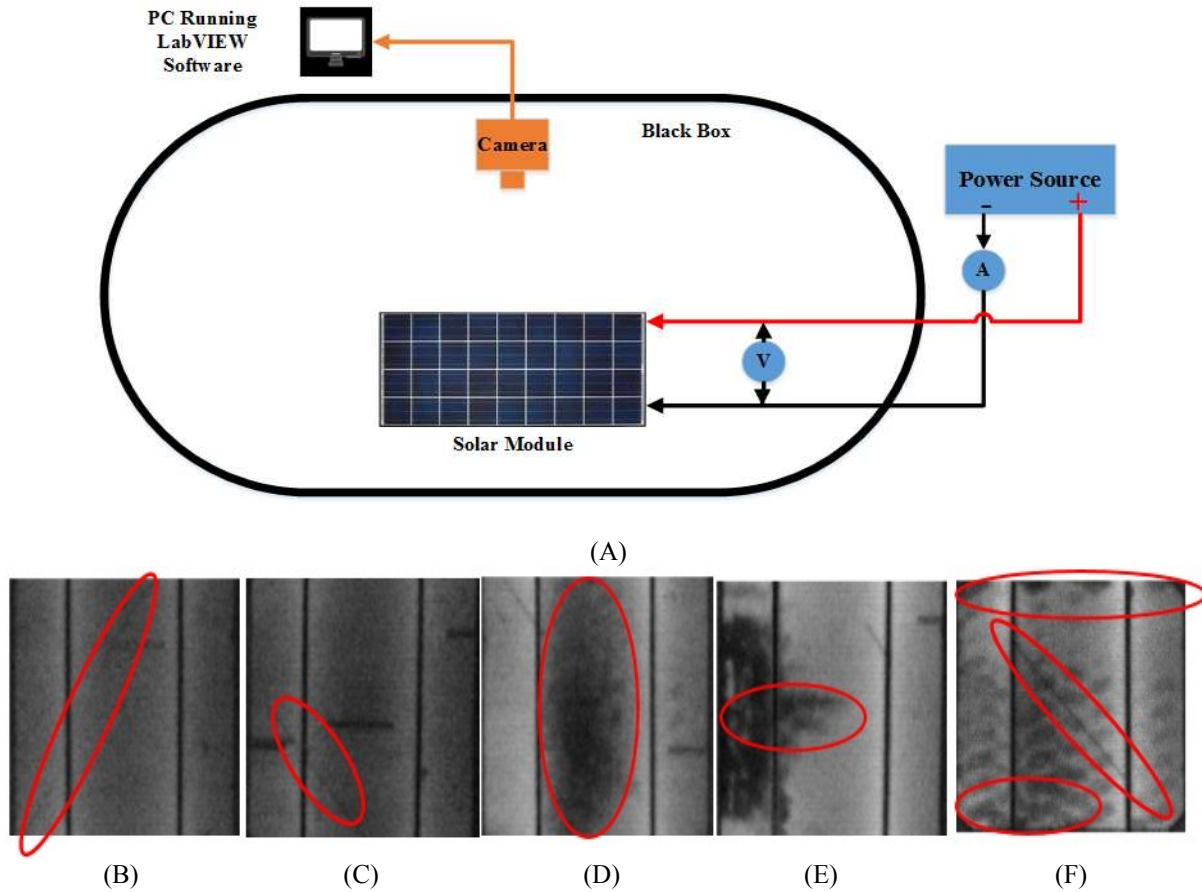


Fig. 2. El Experimental Setup and Examined Crack Types. (A) Electroluminescence experimental setup; (B) Diagonal Crack (+45°); (C) Diagonal Crack (-45°); (D) Parallel to Busbars Crack; (E) Perpendicular to Busbars Crack; (F) Multiple Directions Crack

### 109 2.3. Theoretical output power modelling

110 The DC-Side for all examined PV modules is modelled using 5-parameters model. The voltage  
 111 and the current characteristics of the PV module can be obtained using the single diode model [21]  
 112 as the following:

$$113 \quad I = I_{ph} - I_o \left( e^{\frac{V+IR_s}{nsV_t}} - 1 \right) - \frac{V+IR_s}{R_{sh}} \quad (1)$$

114 Where  $I_{ph}$  is the photo-generated current at STC,  $I_o$  is the dark saturation current at STC,  $R_s$  is  
 115 the module series resistance,  $R_{sh}$  is the panel parallel resistance,  $ns$  is the number of series cells  
 116 in the PV module and  $V_t$  is the thermal voltage and it can be defined based on:

$$117 \quad V_t = \frac{AKT}{q} \quad (2)$$

118 Where  $A$  the diode ideality factor,  $k$  is Boltzmann's constant and  $q$  is the charge of the electron.

119 The five parameters model are determined by solving the transcendental equation (1) using  
 120 Newton-Raphson algorithm. Based only on the datasheet of the available parameters shown  
 121 previously in Table I. The power produced by PV module in watts can be easily calculated along  
 122 with the current (I) and voltage (V) that is generated by equation (1), therefore,  $P_{theoretical} = IV$ .

123 **2.4. Statistical analysis approach**

124 After examining all PV modules which have cracks, a real time simulation can be processed. A  
125 statistical analysis approach is used to determine whether the PV crack has a significant impact on  
126 the total generated output power performance or not. Two statistical methods are used, T-test and  
127 F-test. The first method (T-test) is used to compare the simulated theoretical power with the  
128 measured PV output power. T-test can be evaluated using (3) where  $\bar{x}$  is the mean of the samples,  
129  $\mu$  is the population mean,  $n$  is the sample size and  $SD$  is the standard deviation of the entire data.

130 In this work, we have used a confidence interval for all measured samples equal to 99%.  
131 Statistically speaking, the crack does not have a significant impact on the output power  
132 performance if the t-test value is significant, which means that the t-test value is less than or equal  
133 to 2.58 as shown in Table II.

134 If the t-test value is not significant, another statistical method/layer is used to compare the output  
135 measured power from the cracked PV module with a PV module that has 0% of cracks. This layer  
136 is used to confirm that the output generated power of the cracked PV module has a significant  
137 impact (Real Damage) on the total generated output power performance of the examined  
138 photovoltaic module. In section 4 (results section), most of the inspected results indicates that if  
139 the T-test value is significant, F-test value is also significant. The overall statistical approach can  
140 be explained in Fig. 3 and F-test can be evaluated using (4). The explained variance is calculated  
141 using between groups mean square value, the unexplained variance is calculated using within  
142 groups mean square value [22].

143 Table III, illustrates the expected output results from F-test using 99% (P=0.01) confidence  
144 interval. In this work, an infinite number of samples (Total measured samples > 120) is used to  
145 determine whether the F-test value is significant (F-test  $\leq$  6.635) or not significant (F-test > 6.635).

146 
$$t = \frac{(\bar{x} - \mu)\sqrt{n}}{SD} \quad (3)$$

147 
$$F = \frac{\text{Explained Variance}}{\text{Unexplained Variance}} \quad (4)$$

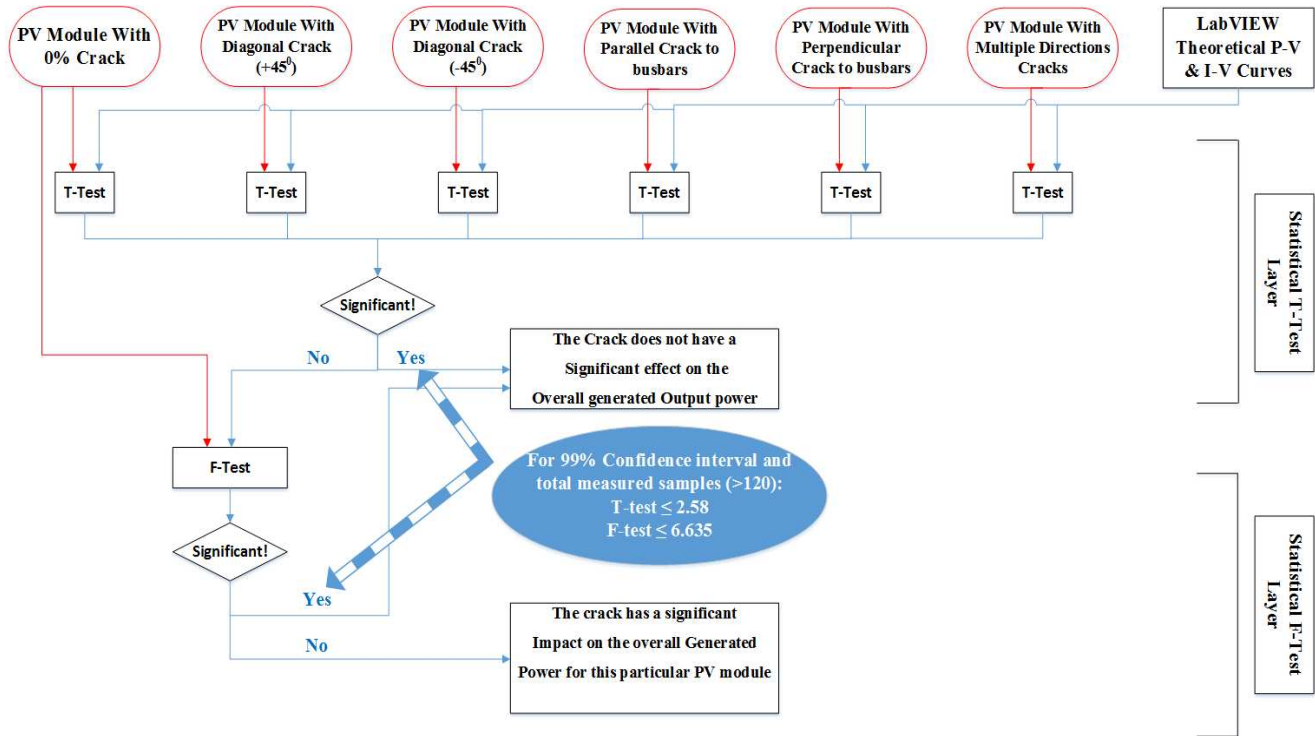


Fig. 3. Statistical Approach Used to Identify Whether the Crack Type has a Significant Impact on the Output Power Performance of a Photovoltaic Module

TABLE II  
STATISTICAL T-TEST CONFIDENCE INTERVAL [22]

Value of t for Confidence Interval of Critical Value  t  for P Values of Number of Degrees of Freedom	90 % (P=0.1)	95% (P=0.05)	99% (P=0.01)
1	6.31	12.71	63.66
20	1.72	2.09	2.85
50	1.68	2.01	2.68
$\infty$	1.64	1.96	2.58

TABLE III  
STATISTICAL F-TEST CRITICAL VALUES FOR 99% CONFIDENCE INTERVAL (p=0.01) [22]

Degree of Freedom (Measured Samples)	Output F-test For a Significant Results
1	4052.181
120	4.787
$\infty$	6.635



149 **3. Results**

150 **3.1. Cracks distribution**

151 As described previously, the statistic micro cracks location, type and size was established by taking  
 152 EL images of 45 PV modules. The EL images are taken with a reflex camera [23]. From the  
 153 captured pictures, the number of cracked cells in each module is counted as shown in Fig. 4.

154 Broken cells are sorted according to the type of crack they show and the classification already  
 155 presented in Fig. 2. The probability for a cell to be cracked and the crack-type distribution are  
 156 presented in Fig. 4. Only 15.556% of the total PV modules have no cracks. However, 84.444% of  
 157 the PV modules contains at least one type of the crack: diagonal (26.666%), parallel to busbars  
 158 (20%), perpendicular to busbars (8.888%) or multiple directions crack (28.888%).

159 According to the statistical approach explained previously in Fig. 3, T-test and F-test methods are  
 160 significant based on a threshold values. Therefore, we have divided all crack-types into two main  
 161 categories:

- 162 • Short: Crack effects one solar cell in a PV module
- 163 • Long: Crack effects two or more solar cell in a PV module

164 Furthermore, fitted line regression is used for the entire measured PV crack-type data. A fitted  
 165 regression represents a mathematical regression equation for the PV measured data. We have  
 166 selected the fitted regression lines to illustrate the relationship between a predictor variable  
 167 (Measured PV Power) and a response variable (Irradiance Level) and to evaluate whether the  
 168 model fits the data. If the measured PV power data is very close to the fitted line regression model,  
 169 therefore, there is a significant relationship between the predictor with the response variable.

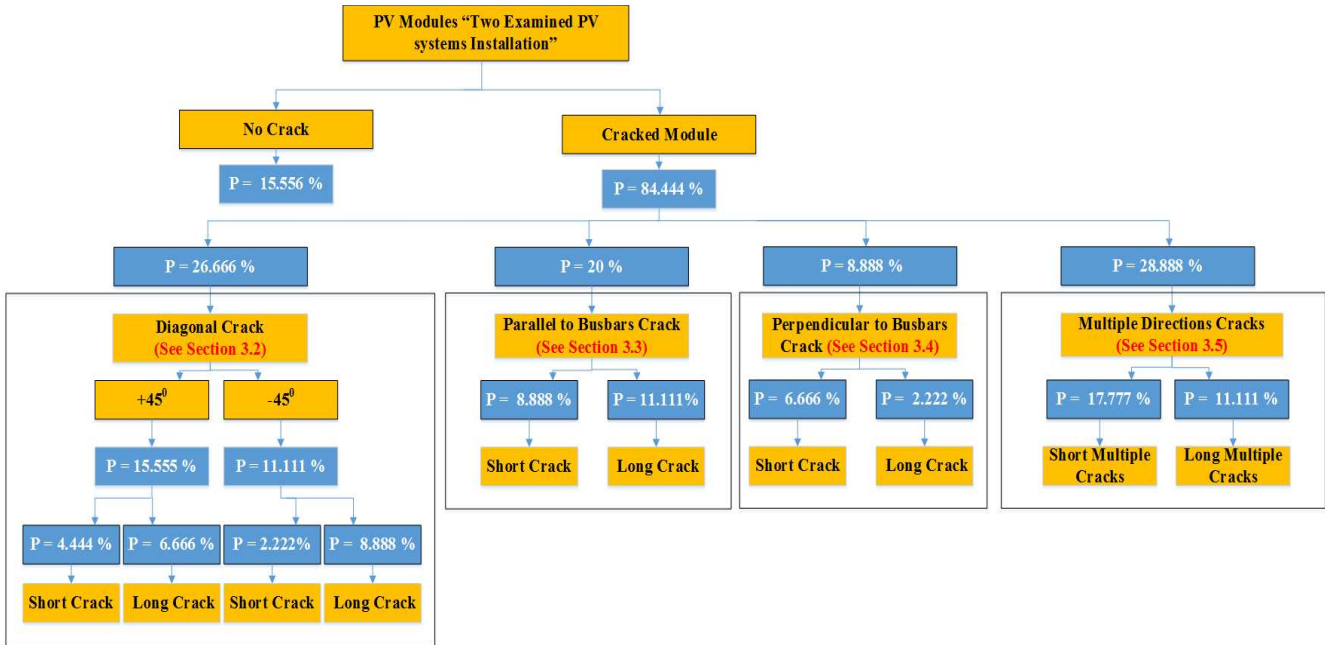


Fig. 4. Crack Types Probability Distribution among Both Examined PV Systems (45 PV Modules)

170 **3.2. Diagonal cracks**

171 Diagonal cracks can be classified into two different categories: +45° and -45° as shown in Fig. 2(A)  
 172 and 2(B) respectively. The measured data which has been carried out from both diagonal crack  
 173 categories indicate that there is a huge similarity in the measured output power performance for  
 174 all examined PV modules. Therefore, we have classified both categories in one crack type. This  
 175 result is different from the results explained in [7, 8] because all the measured data in our  
 176 experiments were taken from a real-time long-term environmental measurements instead of  
 177 laboratory climate conditions.

178 Using the statistical approach, the T-test values for all examined diagonal crack PV modules (12  
 179 PV modules) are shown in Table IV. Since the T-test value for a diagonal crack effects 1 or 2 solar  
 180 cells is less than 99% of the confidence interval threshold (2.58), the output power performance  
 181 for the PV module is statistically not significant: No evidence for a real damage in the PV module.  
 182 The F-test for a diagonal crack effects 1 or 2 solar cells is equal to 4.55 and 5.67 respectively. The  
 183 mathematical expressions for the fitted line regression are illustrated in Table IV.

184 A real-time long-term measured data for a full day is carried out to estimate the output power  
 185 performance for a diagonal crack which effects 1 and 5 solar cells are presented in Fig. 5(A). The  
 186 theoretical simulated output power which is calculated using LabVIEW software has a standard  
 187 deviation equals to 61.46 which is very close to the standard deviation for a diagonal crack which  
 188 effects 1 solar cell (SD=61.38). However, a diagonal crack effects 5 solar cells has a huge reduction  
 189 in the output power performance of the PV module where the standard deviation is equal to 60.99.  
 190 Finally, the measured output power of the PV module matches the theoretical output power,  
 191 therefore, the theoretical power in Fig. 5(A) cannot be seen, this results is also occurring in Fig.  
 192 6(A), Fig. 7(A) and Fig. 8(A).

193 Fig. 5(B) describes the output power efficiency for the examined diagonal cracks effects 1, 2, 3, 4  
 194 and 5 solar cells. Between 0.35 - 0.44% reduction of power estimated for a diagonal crack effects  
 195 1 solar cell. However, the estimated reduction of power for a diagonal crack effects 5 solar cells is  
 196 between 2.97 - 5.37%. The output power efficiency can be estimated using (5).

Table IV  
 Diagonal Cracks Performance Indicators

Diagonal Crack	Number of Effected Solar Cells	Approximate Area Broken (mm)	T-test Value	Significant/Not Significant Effect on the PV Power Performance	Fitted Line Regression Equation
Short +45° OR Short -45°	1	1 mm <sup>2</sup> – 83 mm <sup>2</sup>	0.40 - 0.66	<b>Not Significant</b>	$P_{TH} = 0.1424 + 1.001 P_{Meas}$
Long +45° OR Long -45°	2	85.85 mm <sup>2</sup> – 169.7 mm <sup>2</sup>	1.22 – 1.86	<b>Not Significant</b>	$P_{TH} = 0.2875 + 1.003 P_{Meas}$
	3	172.7 mm <sup>2</sup> - 256.6 mm <sup>2</sup>	2.51 - 2.71	Significant	$P_{TH} = 0.5125 + 1.006 P_{Meas}$
	4	257. 5 mm <sup>2</sup> - 344.4 mm <sup>2</sup>	2.65 – 2.70	Significant	$P_{TH} = 0.7034 + 1.008 P_{Meas}$
	5	345.1 mm <sup>2</sup> – 424.3 mm <sup>2</sup>	3.12 – 3.35	Significant	$P_{TH} = 1.151 + 1.013 P_{Meas}$

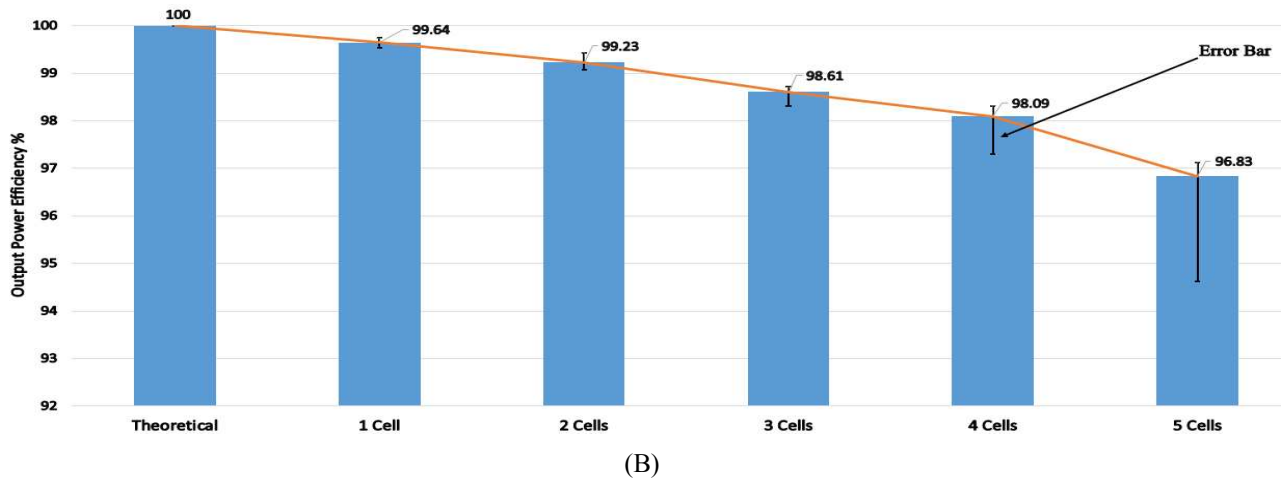
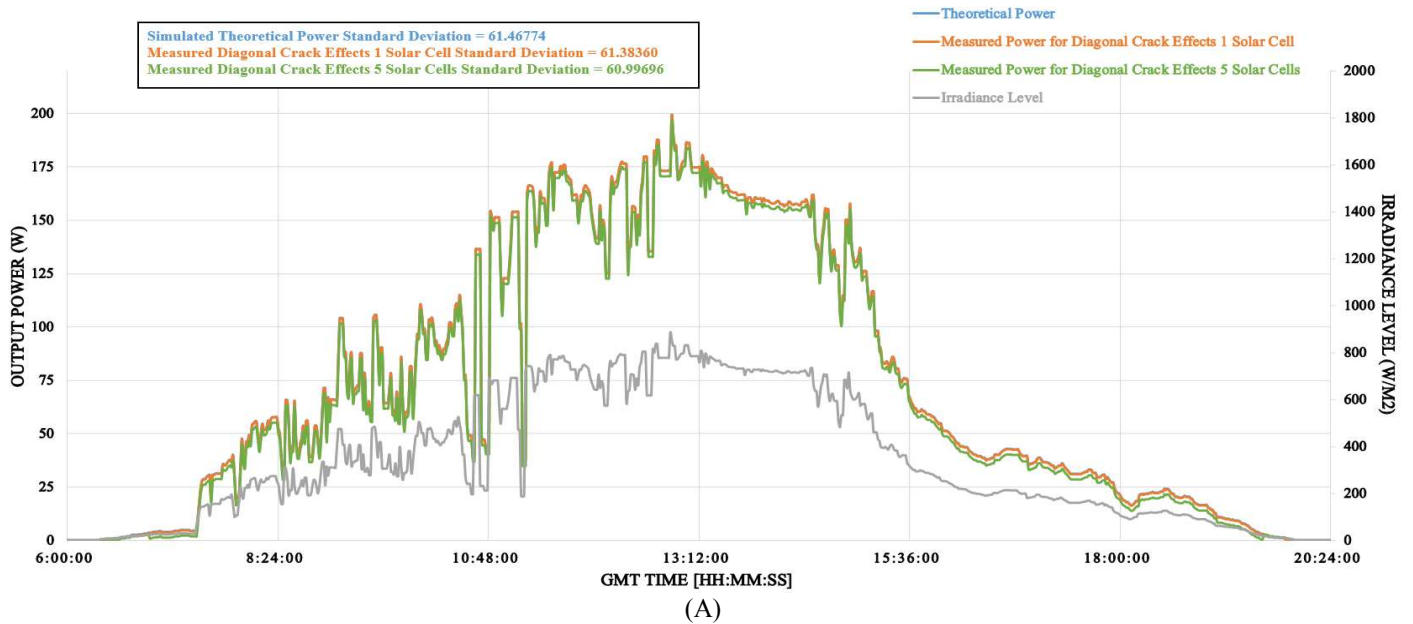


Fig. 5. (A) Real-Time Long-Term Measured Data for a Diagonal Crack Effects 1 and 5 Solar Cells; (B) Output Power Efficiency for a Diagonal Cracks Which Effects 1, 2, 3, 4 and 5 PV Solar Cells

### 197 3.3. Parallel to busbars cracks

198 As explained previously in Fig. 5, parallel to the busbars cracks has a percentage of occurrence  
 199 20% (9 PV modules out of 45 examined PV modules) and they are listed as the following:

- 200 • 8.888% (4 PV modules): Short Crack Effect
- 201 • 11.111% (5 PV modules): Long Crack Effect

202 Not all parallel to busbars cracks has a significant impact/reduction on the output power  
 203 performance of the PV module. As shown in Table V, parallel to busbars cracks effects 1 solar cell  
 204 statistically indicates that there is no real damage in the PV module, the result is confirmed by the  
 205 T-test value which is less than the threshold value 2.58. Moreover, when a parallel to busbars crack  
 206 effects 2 solar cells with approximate broken area less than 82mm<sup>2</sup> have no significant effect on  
 207 the amount of power generated by the PV module. Additionally, Table V illustrates various

208 mathematical equations for the measured fitted line regression which describes the relationship  
 209 between the theoretical and measured output power.

210 Fig. 6(A) presents real-time measured data for a parallel to busbars crack effects 1 and 4 solar  
 211 cells. The standard deviation for the theoretical simulated power is 62.01 which is very close to  
 212 the standard deviation for a parallel to busbars crack effects 1 solar cell (61.8). However, parallel  
 213 to busbars crack effects 5 solar cells has a huge reduction in the output power performance of the  
 214 PV module while the standard deviation is equal to 61.09.

215 Fig. 6(B) describes the output power efficiency for the examined parallel to busbars cracks effects  
 216 1, 2, 3 and 4 solar cells. The reduction of power estimated for a parallel to busbars crack effects 1  
 217 solar cell is between 0.75% - 0.97%. However, the estimated reduction of power for a parallel to  
 218 busbars crack effects 3 and 4 solar cells is between 2.39% - 3.0% and 3.67% - 4.55% respectively.

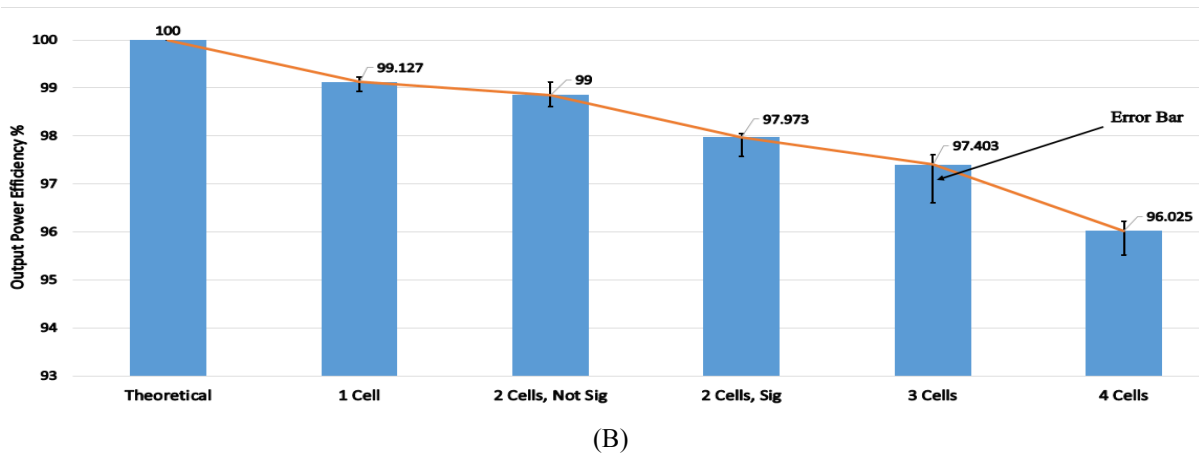
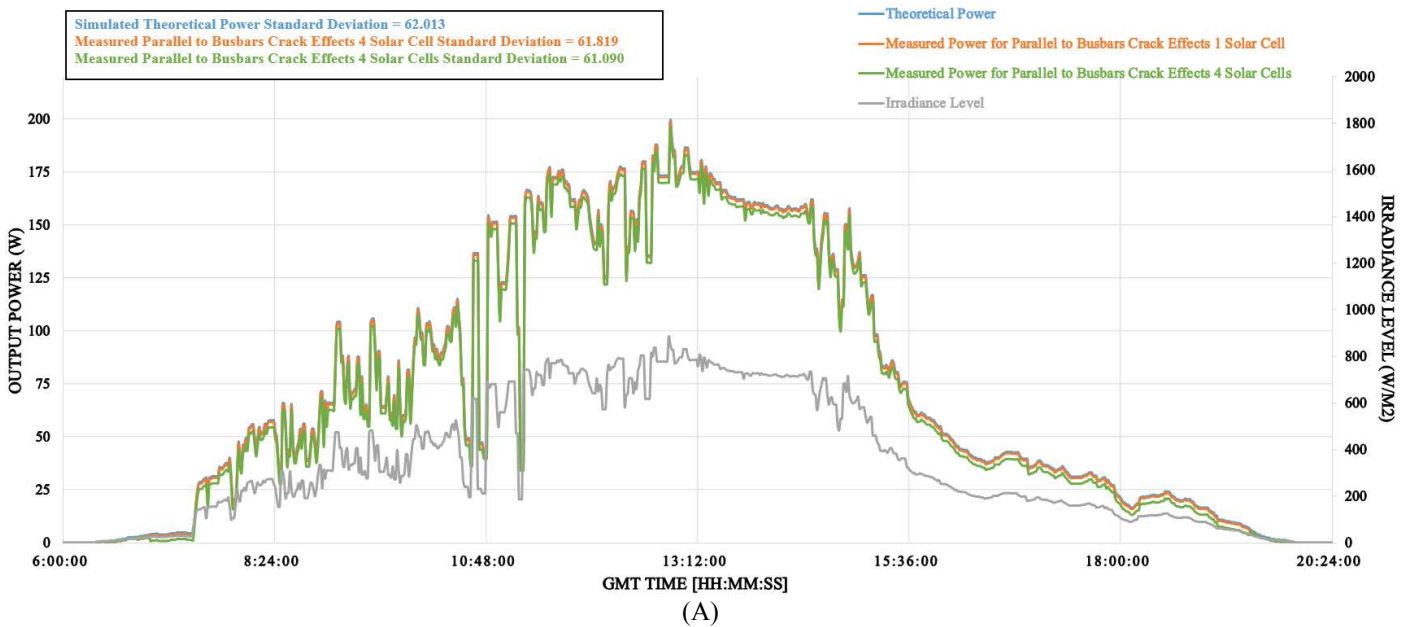


Fig. 6. (A) Real-Time Long-Term Measured Data for a Parallel to Busbars Crack Which Effects 1 and 4 Solar Cells; (B) Output Power Efficiency for Parallel to Busbars Crack Which Effects 1, 2, 3 and 4 PV Solar Cells

$$Efficiency = \frac{Measured\ Output\ Power}{Theoretical\ Output\ Power} \times 100\% \quad (5)$$

Table V  
Parallel to Busbars Cracks Performance Indicators

Crack Type		Number of Effected Solar Cells	Approximate Area Broken (mm)	T-test Value	Significant/Not Significant Effect on the PV Power Performance	Fitted Line Regression Equation
Parallel To Busbars	Short	1	1 mm <sup>2</sup> – 59.2 mm <sup>2</sup>	0.78 – 1.13	<b>Not Significant</b>	$P_{TH} = 0.3002 + 1.001 P_{Meas}$
	Long	2	63 mm <sup>2</sup> – 81 mm <sup>2</sup>	1.42 – 1.87	<b>Not Significant</b>	$P_{TH} = 0.3990 + 1.004 P_{Meas}$
			82 mm <sup>2</sup> – 121 mm <sup>2</sup>	2.62 – 2.74	Significant	$P_{TH} = 0.6923 + 1.008 P_{Meas}$
		3	122 mm <sup>2</sup> – 177 mm <sup>2</sup>	4.04 – 4.81	Significant	$P_{TH} = 0.9218 + 1.010 P_{Meas}$
		4	177.3 mm <sup>2</sup> – 239.7 mm <sup>2</sup>	4.39 – 5.66	Significant	$P_{TH} = 1.3590 + 1.016 P_{Meas}$

### 219 3.4. Perpendicular to busbars cracks

220 Perpendicular to busbars cracks usually do not occur in PV modules. In research have  
 221 distinguished only 4 PV modules from 45 to be classified as a perpendicular to busbars cracks.  
 222 This result has been verified by many articles such as [7, 8]. Table VI shows all numerical results  
 223 which are measured from the examined PV modules.

224 Table VI indicates that a perpendicular to busbars crack effects 1, 2 and 3 busbars statistically has  
 225 no significant impact on the overall amount of power produced by a PV module. The measured  
 226 results for a perpendicular to busbars cracks effects 1 and 4 solar cells can be seen in Fig. 7 (A),  
 227 the difference between the theoretical standard deviation and a perpendicular to busbars cracks  
 228 which effects 4 solar cells is equal to 1.014. Finally, Fig. 7(b) illustrates the output power efficiency  
 229 measured for a perpendicular to busbars which effects 1, 2, 3 and 4 solar cells (1-8 Busbars), where  
 230 the maximum power reduction is estimated for 8 busbars between 4.6 – 4.1%.

Table VI  
Perpendicular to Busbars Cracks Performance Indicators

Crack Type		Number of Effected Solar Cells	Number of Effected Busbars	Approximate Area Broken (mm)	T-test Value	Significant/Not Significant Effect on the PV Power Performance	Fitted Line Regression Equation
Perpendicular To Busbars	Short	1	1	1 mm <sup>2</sup> – 16.2 mm <sup>2</sup>	0.65 – 0.82	<b>Not Significant</b>	$P_{TH} = 0.0927 + 1.001 P_{Meas}$
			2	16.3 mm <sup>2</sup> – 60 mm <sup>2</sup>	0.92 – 1.31	<b>Not Significant</b>	$P_{TH} = 0.1524 + 1.002 P_{Meas}$
	Long	2	3	61.3 mm <sup>2</sup> – 78.5 mm <sup>2</sup>	1.43 – 1.96	<b>Not Significant</b>	$P_{TH} = 0.3604 + 1.004 P_{Meas}$
			4	79.4 mm <sup>2</sup> – 120 mm <sup>2</sup>	2.52 – 2.77	Significant	$P_{TH} = 0.4678 + 1.005 P_{Meas}$
		3	5	120.5 mm <sup>2</sup> – 137.4 mm <sup>2</sup>	2.83 – 2.94	Significant	$P_{TH} = 0.7397 + 1.008 P_{Meas}$
			6	138 mm <sup>2</sup> – 179.8 mm <sup>2</sup>	2.79 – 3.11	Significant	$P_{TH} = 0.9265 + 1.010 P_{Meas}$
		4	7	181.5 mm <sup>2</sup> – 195 mm <sup>2</sup>	3.02 – 3.27	Significant	$P_{TH} = 1.0790 + 1.012 P_{Meas}$
			8	196.2 mm <sup>2</sup> – 240.2 mm <sup>2</sup>	3.10 – 3.55	Significant	$P_{TH} = 1.4590 + 1.018 P_{Meas}$

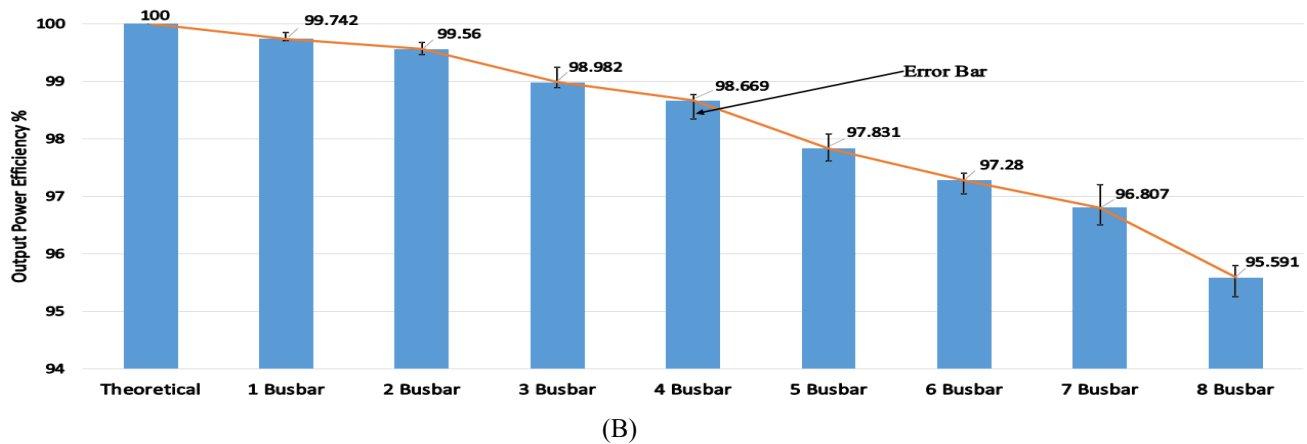
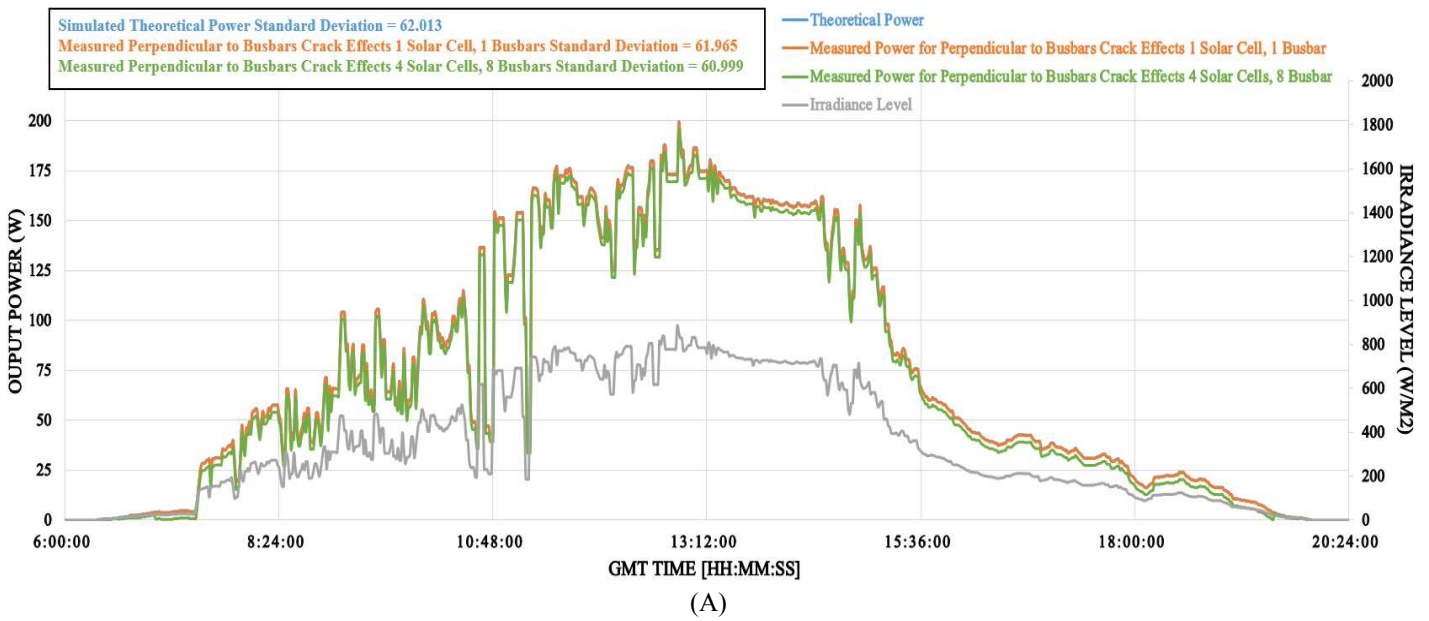


Fig. 7. (A) Real-Time Long-Term Measured Data for a Perpendicular to Busbars Crack Effects 1 and 4 Solar Cells; (B) Output Power Efficiency for a Perpendicular to Busbars Crack Which Effects 1, 2, 3 and 4 (1-8 busbars) PV Solar Cells

231 **3.5. Multiple directions crack**

232 Multiple directions cracks have the highest degradation in the PV measured output power. Three  
 233 different measured data are presented in Fig. 8(A). As illustrated in Fig. 8(B), multiple directions  
 234 crack effects 5 solar cells reduce the power efficiency of the PV module up to 8.42%. However,  
 235 the average reduction in the power for a multiple directions crack effects 1 solar cell with an  
 236 approximate broken area less than 46.2 mm<sup>2</sup> is equal to 1.04%.

237 Table VII shows a brief explanation for the T-test values and whether a multiple directions crack  
 238 has a significant or not significant impact on the total output power produced by a cracked PV  
 239 module.

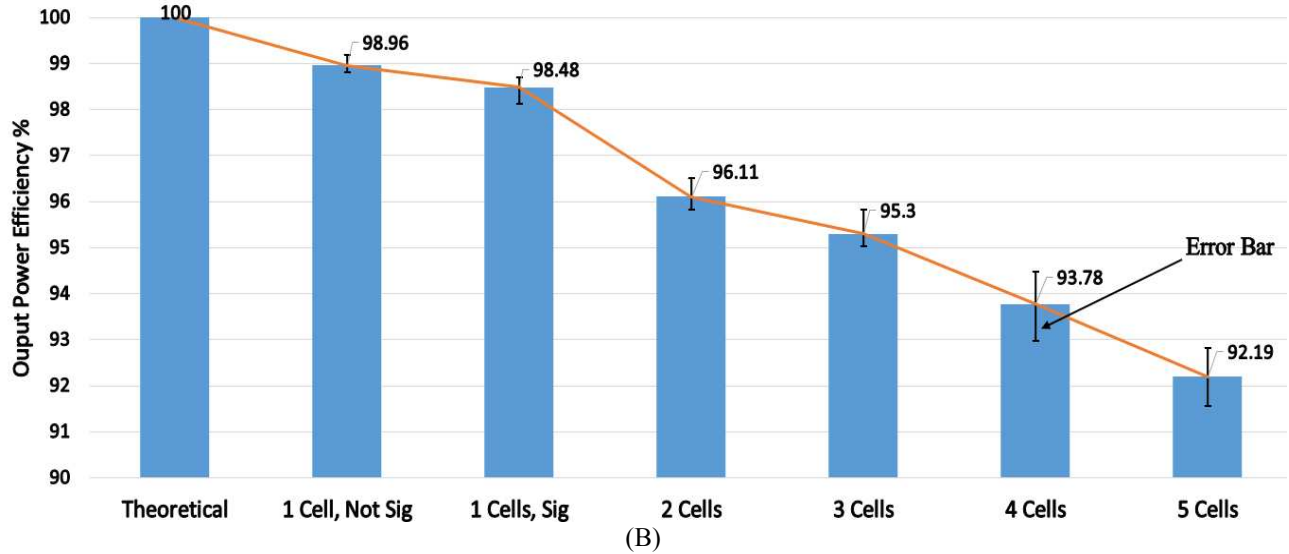
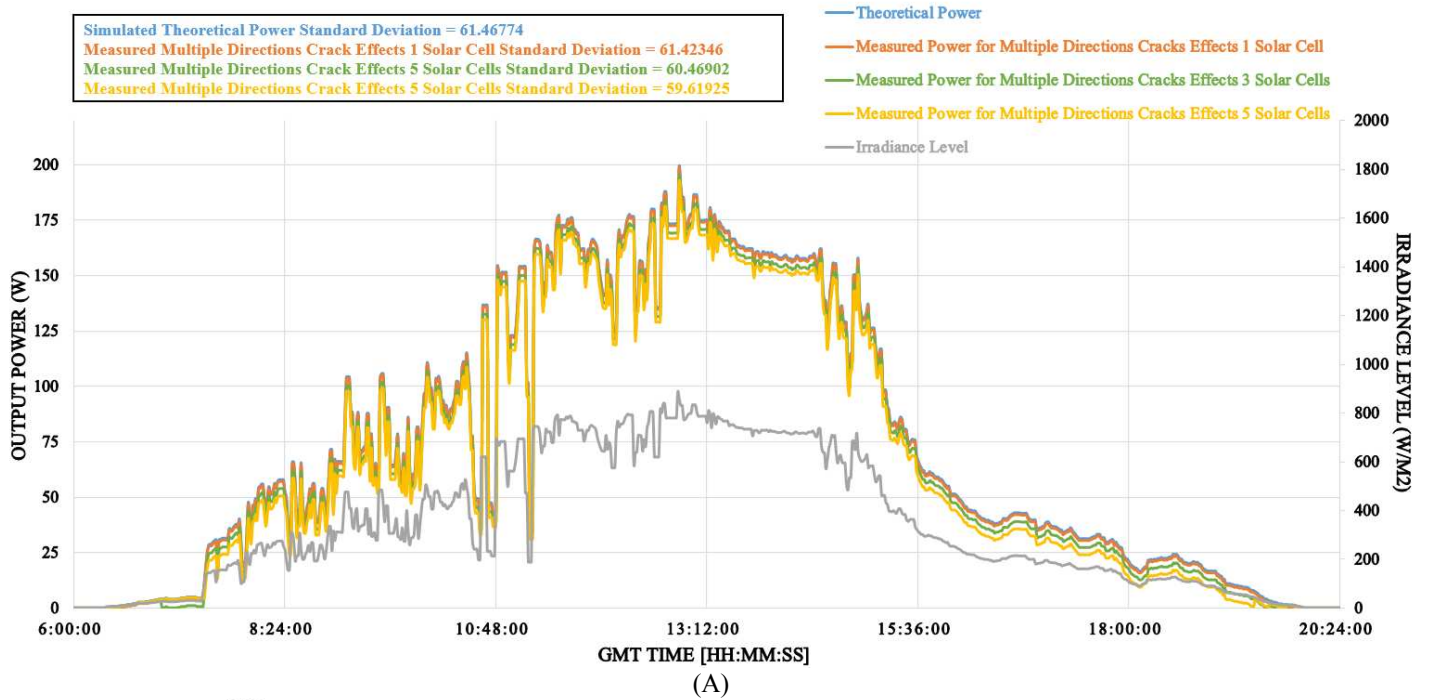


Fig. 8. (A) Real-Time Long-Term Measured Data for a Multiple Directions Crack Effects on 1, 3 and 5 Solar Cells; (B) Output Power Efficiency for a Multiple Directions Crack Which Effects 1,2,3,4 and 5 PV Solar Cells

Table VII  
Multiple Directions Cracks Performance Indicators

	Number of Effected Solar Cells	Approximate Area Broken (mm)	T-test Value	Significant/Not Significant Effect on the PV Power Performance	Fitted Line Regression Equation
Multiple Directions Crack	1	1 mm <sup>2</sup> – 45 mm <sup>2</sup>	2.06 – 2.44	<b>Not Significant</b>	$P_{TH} = 0.3679 + 1.004 P_{Meas}$
		46.2 mm <sup>2</sup> – 1000 mm <sup>2</sup>	2.68 – 2.88	Significant	$P_{TH} = 0.5330 + 1.005 P_{Meas}$
	2	100 mm <sup>2</sup> – 3700 mm <sup>2</sup>	3.25 – 3.33	Significant	$P_{TH} = 1.028 + 1.012 P_{Meas}$
	3	170 mm <sup>2</sup> – 5000 mm <sup>2</sup>	4.70 – 4.88	Significant	$P_{TH} = 1.554 + 1.019 P_{Meas}$
	4	223 mm <sup>2</sup> – 8200 mm <sup>2</sup>	6.17 – 6.31	Significant	$P_{TH} = 2.015 + 1.027 P_{Meas}$
	5	400 mm <sup>2</sup> – 9800 mm <sup>2</sup>	7.30 – 7.52	Significant	$P_{TH} = 2.577 + 1.033 P_{Meas}$

240 **4. Discussion**

241 **4.1. Overall cracks assessment**

242 The observed modules have 38 PV modules with various crack-types. The probability of  
 243 occurrence for each crack type can be seen in Fig. 4. Before considering the statistical approach,  
 244 it is hypothetically true to say that 84.4% has a significant impact on the output power performance.  
 245 However, the statistical approach has confirmed that this is incorrect, because only 60% has a  
 246 significant impact on the output power performance for all examined PV modules.

247 This result can be investigated further more by applying the same statistical approach on various  
 248 PV systems in different regions around the world. The only difference might be the confidence  
 249 interval limitations (99%, 95% and 90%) due to the various accuracy rates for the instrumentation  
 250 used in the PV systems such as the Voltage sensors, Current sensors and Temperature sensors.

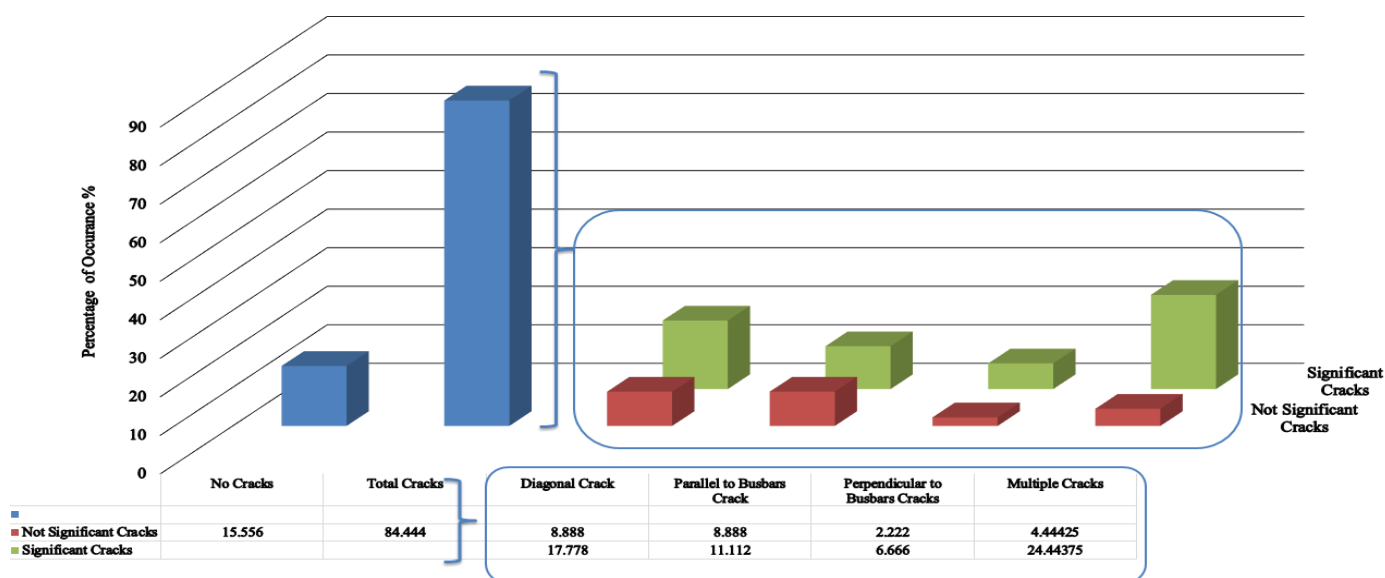


Fig. 19. Percentage of Cracks in the Examined PV modules, overall significant Cracks equals to 60% out of 84.444%

251 **4.2 Surface damage**

252 For better understanding how some cracks effects the surface of the PV modules, we have created  
 253 a MATLAB code which can simulate the measured data of a cracked PV module in order to  
 254 evaluate the surface shape for a particular crack-type using Surf(x, y, z) MATLAB function [24].

255 Fig. 10(A) shows a diagonal crack (+45°) effects 3 solar cells. It is clear that the surface of three  
 256 different solar cells are damaged (Noted as 1, 2 and 3). The degradation of the power for the solar  
 257 cells is between 0.5 and 1 Watt. Overall PV module efficiency can be estimated by the MATLAB  
 258 code which is equal to 98.61%, this result can be illustrated in Figs. 5(B) and 10(A).

259 Similarly, Fig 10(B) describes the surface shape of a parallel to busbars crack which effects 3 solar  
 260 cells. The degradation of the power in the affected solar cells is between 2.5 and 2 Watt. The



261 overall power efficiency of the PV module is equal to 97.41% which is very similar to the value  
 262 (97.4%) described earlier in Fig. 6(B).

263 The surface shape for a perpendicular to busbars crack effects 3 solar cells, 6 Busbars is illustrated  
 264 in Fig. 10(C). However, Fig. 10(D) shows a cracked surface for a PV module that is affected by a  
 265 multiple directions crack on 3 different solar cells. Moreover, a perpendicular crack effects a solar  
 266 cell with 2 busbars has an estimated degradation of power equals to 1.5 Watt. Overall efficiency  
 267 of the cracked surfaces is equal to 97.28% for a perpendicular to busbars crack which effects 3  
 268 solar cells (6 busbars), and 95.3% for a multiple directions crack which effects 3 solar cells.

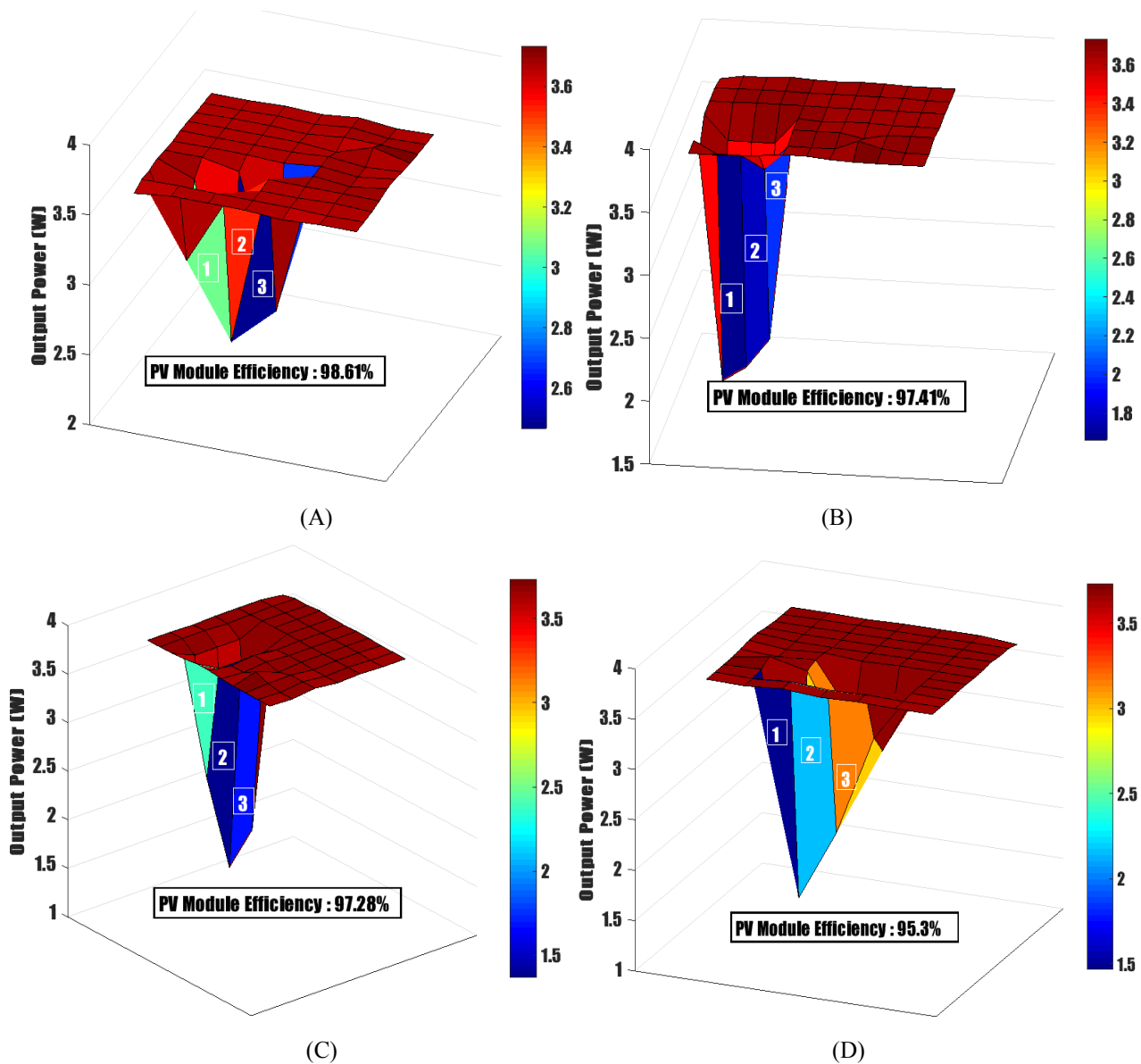


Fig. 10. (A) Surface Shape for a Diagonal (+45°) Crack Effects 3 Solar Cells; (B) Surface Shape for a Parallel to Busbars Crack Effects 3 Solar Cells (C) Surface Shape for a Perpendicular to Busbars Crack Effects 3 Solar Cells, 6 Busbars; (D) Surface Shape for a Multiple Directions Crack Effects 3 Solar Cells

## 269 **5. Conclusion**

270 This paper propose a new statistical algorithm to identify the significant of the cracks on the output  
271 power performance of the PV modules. The algorithm is developed using a Virtual Instrumentation  
272 (VI) LabVIEW software. We have examined 45 PV modules with various crack-type such as  
273 diagonal, parallel to busbars, perpendicular to busbars and multiple directions crack.

274 Before considering the statistical approach, 84.44% of the examined PV modules have a significant  
275 impact on the output power performance. However, the statistical approach has confirmed that this  
276 result is incorrect, since only 60% of the examine PV cracks have a significant impact on the output  
277 power performance.

278 Based on the measured output power data of each crack-type PV module, we have evaluated the  
279 fitted line regression equations. Subsequently, the surface of cracked PV modules have been  
280 demonstrated using Surf(x, y, z) MATLAB Function.

281 For further work, we are designing a generic algorithm based on statically analysis techniques to  
282 detect multiple faults in PV systems such as DC-Side faults, AC-Side faults, PV cracks and shading  
283 effect.

## 284 **6. Acknowledgment**

285 Authors would like to acknowledge the financial assistant to the University of Huddersfield,  
286 Engineering and Computing Department.

## 287 **References**

288 [1] Rajput, P., Tiwari, G. N., Sastry, O. S., Bora, B., & Sharma, V. (2016). Degradation of mono-  
289 crystalline photovoltaic modules after 22years of outdoor exposure in the composite climate of  
290 India. *Solar Energy*, 135, 786-795.

291 [2] Dhimish, M., Holmes, V., & Dales, M. (2016, September). Grid-connected PV virtual  
292 instrument system (GCPV-VIS) for detecting photovoltaic failure. In *Environment Friendly*  
293 *Energies and Applications (EFEA), 2016 4th International Symposium on* (pp. 1-6). IEEE.

294 [3] Sharma, V., & Chandel, S. S. (2013). Performance and degradation analysis for long term  
295 reliability of solar photovoltaic systems: a review. *Renewable and Sustainable Energy Reviews*, 27,  
296 753-767.

297 [4] Köntges, M., Kunze, I., Kajari-Schröder, S., Breitenmoser, X., & Bjørneklett, B. (2010,  
298 September). Quantifying the risk of power loss in PV modules due to micro cracks. In *25th*  
299 *European Photovoltaic Solar Energy Conference, Valencia, Spain* (pp. 3745-3752).

300 [5] Kajari-Schröder, S., Kunze, I., Eitner, U., & Köntges, M. (2011). Spatial and orientational  
301 distribution of cracks in crystalline photovoltaic modules generated by mechanical load tests. *Solar*  
302 *Energy Materials and Solar Cells*,95(11), 3054-3059.

- 303 [6] Dallas, W., Polupan, O., & Ostapenko, S. (2007). Resonance ultrasonic vibrations for crack  
304 detection in photovoltaic silicon wafers. *Measurement Science and Technology*, 18(3), 852.
- 305 [7] Morlier, A., Haase, F., & Köntges, M. (2015). Impact of cracks in multicrystalline silicon solar  
306 cells on PV module power—A simulation study based on field data. *IEEE Journal of*  
307 *Photovoltaics*, 5(6), 1735-1741.
- 308 [8] Paggi, M., Corrado, M., & Rodriguez, M. A. (2013). A multi-physics and multi-scale numerical  
309 approach to microcracking and power-loss in photovoltaic modules. *Composite Structures*, 95,  
310 630-638.
- 311 [9] Köntges, M., Kajari-Schröder, S., Kunze, I., & Jahn, U. (2011, September). Crack statistic of  
312 crystalline silicon photovoltaic modules. In *26th European Photovoltaic Solar Energy Conference*  
313 *and Exhibition* (pp. 5-6).
- 314 [10] van Mülken, J. I., Yusufoglu, U. A., Safiei, A., Windgassen, H., Khandelwal, R., Pletzer, T.  
315 M., & Kurz, H. (2012). Impact of micro-cracks on the degradation of solar cell performance based  
316 on two-diode model parameters. *Energy Procedia*, 27, 167-172.
- 317 [11] Kaplani, E. (2016, April). Degradation in Field-aged Crystalline Silicon Photovoltaic  
318 Modules and Diagnosis using Electroluminescence Imaging. In *Presented at 8th International*  
319 *Workshop on Teaching in Photovoltaics (IWTPV'16)* (Vol. 7, p. 8).
- 320 [12] Munoz, M. A., Alonso-Garcia, M. C., Vela, N., & Chenlo, F. (2011). Early degradation of  
321 silicon PV modules and guaranty conditions. *Solar energy*, 85(9), 2264-2274.
- 322 [13] Gerber, A., Huhn, V., Tran, T. M. H., Siegloch, M., Augarten, Y., Pieters, B. E., & Rau, U.  
323 (2015). Advanced large area characterization of thin-film solar modules by electroluminescence  
324 and thermography imaging techniques. *Solar Energy Materials and Solar Cells*, 135, 35-42.
- 325 [14] Köntges, M., Siebert, M., Hinken, D., Eitner, U., Bothe, K., & Potthof, T. (2009, September).  
326 Quantitative analysis of PV-modules by electroluminescence images for quality control. In *24th*  
327 *European Photovoltaic Solar Energy Conference, Hamburg, Germany* (pp. 21-24).
- 328 [15] Berardone, I., Corrado, M., & Paggi, M. (2014). A generalized electric model for mono and  
329 polycrystalline silicon in the presence of cracks and random defects. *Energy Procedia*, 55, 22-29.
- 330 [16] Spataru, S., Hacke, P., Sera, D., Glick, S., Kerekes, T., & Teodorescu, R. (2015, June).  
331 Quantifying solar cell cracks in photovoltaic modules by electroluminescence imaging.  
332 In *Photovoltaic Specialist Conference (PVSC), 2015 IEEE 42nd* (pp. 1-6). IEEE.
- 333 [17] Dhimish, M., Holmes, V., & Dales, M. (2016, September). Grid-connected PV virtual  
334 instrument system (GCPV-VIS) for detecting photovoltaic failure. In *Environment Friendly*  
335 *Energies and Applications (EFEA), 2016 4th International Symposium on* (pp. 1-6). IEEE.
- 336 [18] Dhimish, M., & Holmes, V. (2016). Fault detection algorithm for grid-connected photovoltaic  
337 plants. *Solar Energy*, 137, 236-245.

- 338 [19] Silvestre, S., Chouder, A., & Karatepe, E. (2013). Automatic fault detection in grid connected  
339 PV systems. *Solar Energy*, 94, 119-127.
- 340 [20] Kajari-Schröder, S., Kunze, I., Eitner, U., & Köntges, M. (2011). Spatial and orientational  
341 distribution of cracks in crystalline photovoltaic modules generated by mechanical load tests. *Solar*  
342 *Energy Materials and Solar Cells*, 95(11), 3054-3059.
- 343 [21] McEvoy, A., Castaner, L., Markvart, T., 2012. *Solar Cells: Materials, Manufacture and*  
344 *Operation*. Academic Press.
- 345 [22] Miller, J. N., & Miller, J. C. (2010; 2011). *Statistics and chemometrics for analytical*  
346 *chemistry* (6th ed.). Harlow: Prentice Hall.
- 347 [23] Köntges, M., Kajari-Schröder, S., & Kunze, I. (2013). Crack statistic for wafer-based silicon  
348 solar cell modules in the field measured by UV fluorescence. *IEEE Journal of Photovoltaics*, 3(1),  
349 95-101.
- 350 [24] Guo, G., Luc, S., Marco, E., Lin, T. W., Peng, C., Kerényi, M. A., ... & Neff, T. (2013).  
351 Mapping cellular hierarchy by single-cell analysis of the cell surface repertoire. *Cell stem*  
352 *cell*, 13(4), 492-505.